

Single-parameter charge pump in a zigzag graphene nanoribbon

This article has been downloaded from IOPscience. Please scroll down to see the full text article.

2009 J. Phys.: Condens. Matter 21 405301

(<http://iopscience.iop.org/0953-8984/21/40/405301>)

View [the table of contents for this issue](#), or go to the [journal homepage](#) for more

Download details:

IP Address: 129.252.86.83

The article was downloaded on 30/05/2010 at 05:31

Please note that [terms and conditions apply](#).

Single-parameter charge pump in a zigzag graphene nanoribbon

Y Gu¹, Y H Yang¹, J Wang^{1,2} and K S Chan²

¹ Department of Physics, Southeast University, Nanjing 210096, People's Republic of China

² Department of Physics and Materials Science, City University of Hong Kong, Tat Chee Avenue, Kowloon, Hong Kong, People's Republic of China

E-mail: ygu@seu.edu.cn and apkschan@cityu.edu.hk

Received 30 June 2009, in final form 14 August 2009

Published 8 September 2009

Online at stacks.iop.org/JPhysCM/21/405301

Abstract

We report a theoretical study of a single-parameter quantum charge pump in the clean zigzag graphene nanoribbon (ZGNR) system. By Keldysh Green's function method, we show that a pumped current in the ZGNR with an even number of zigzag chains can sharply increase from zero as the frequency matches the Fermi energy, whereas the pumped charge current is always absent in the ZGNR with an odd number of zigzag chains as well as the GNR with armchair edges, it is attributed to the peculiar zero-energy edge state in the ZGNR and the symmetry breaking of the topologically inequivalent carbon atoms due to the zigzag edges. The pumped current in the even-ZGNR decreases with the Fermi energy and its direction is determined by Fermi energy below or above the Dirac point as well as the type of carbon atoms at one edge of the ZGNR. The two-parameter charge pump in the ZGNR is also discussed and the magnitude of the pumped current is comparable to the single-parameter pump when the pumping frequency matches the Fermi energy.

(Some figures in this article are in colour only in the electronic version)

1. Introduction

Since the successful realization of a two-dimensional monolayer of carbon atoms [1–3], graphene has drawn an explosion of interest in global scientific communities in recent years. Graphene represents a one-atom-thick layer of carbon atoms tightly packed into a honeycomb crystal lattice whose symmetries impose a linear energy–momentum dispersion on the low-energy quasiparticles, which can be described by the massless relativistic Dirac equation [4–6]. This linear dispersion of graphene has led to far-reaching results, e.g., the specular Andreev reflection [6] in a normal/superconductor junction, Klein tunneling [7] related to the chiral nature of the quasiparticle; other interesting phenomenons include the unconventional half-integer quantum Hall effect [8, 9], a bipolar supercurrent [10], and the realization of superlenses by focusing of electron beams [11].

Graphene has a very long mean-free-path and spin coherence lengths, as well as a high carrier mobility, that can be 30 times that in 2DEG of the GaAs heterostructure, so graphene-based electronic devices are expected to possess many advantages over traditional Si-based electronic

devices [1–3]. The electron and spin transport property of graphene has drawn much attention from researchers since it is important for the fabrication of electronic devices. In a nanoscale graphene or graphene nanoribbon (GNR), the transport is expected to depend strongly on whether they have an armchair or zigzag edge. In a GNR with zigzag edges (ZGNR), the transport is dominated by the edge state [12–14] which has been observed in scanning tunneling microscopy [15]. Due to existence of two edges, the energy bands of the ZGNR become so flat at the Dirac point that an energy gap can be induced, and even a spin-polarized state, the flat energy band at Dirac point leads to a very sharp peak of the density of states that corresponds to electronic states localized in the near vicinity of the two edges. The physical origin is that two topologically inequivalent carbon atoms locate at two edges so that non-bonding states can form at two edges and decay from the edge to the inner part of the ZGNR.

The edge state of the ZGNR can be regarded as spontaneous symmetry breaking between two inequivalent carbon atoms due to two edges, (compared with bulk graphene, the ZGNR does not have bulk inversion symmetry), which may have an effect on the equilibrium transport properties; for

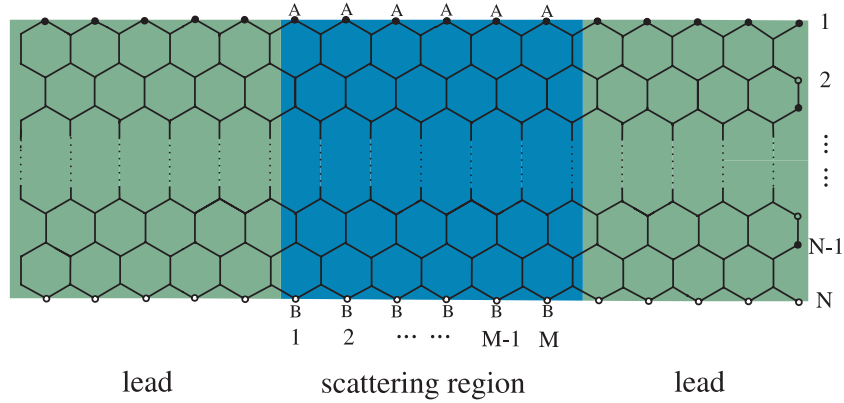


Figure 1. The schematic structure of a uniform graphene nanoribbon with a zigzag edge. A and B type carbon atoms are at the upper and lower edge, respectively, the number of the zigzag chains N is even. The shadow part $N \times M$ is the scattering region where the pumping potentials are applied, the other two regions are set as the left and right ideal lead, N is the zigzag chain number along the transverse direction while M is the unit slice index in the scattering region.

instance, the equilibrium supercurrent in a Josephson junction comes from the symmetry breaking of the superconductor macroscopic phase. The quantum parametric pump [16] in a mesoscopic system at zero bias also comes from the symmetry breaking of the parameter space. A quantum pump is a device capable of providing a charge current without any bias and typically involves the cyclic change of two or more time-dependent parameters with a nonvanishing phase difference between them. For a single-parameter charge pump the time-dependent parameters are in the same phase, it is also probable to pump out the charge current when the system including the pumping points does not possess spatial inversion symmetry (SIS), e.g., Wang *et al* [17] found that when the device with a single pumping point possesses SIS, there is no pumped current, whereas the device without SIS can pump out a nonzero charge current and the pumped current is proportional to the frequency squared ω^2 . Torres [18] employed a magnetic field to destroy the SIS of a quantum ring device and in that case the single-parameter charge pump can work.

Since the edge state in the ZGNR reflects the symmetry breaking between two inequivalent carbon atoms (say, one edge is composed of A carbon atoms and the other edge must be from B carbon atoms as shown in figure 1), it is worth studying the charge pump effect in the ZGNR system, especially, the single-parameter charge pump. Thus in this work, we study the single-parameter pump in a finite ZGNR with an even number of zigzag chains in a device as shown in figure 1, the charge pumping potential can be in principle realized by a top gate that is capacitively coupled to the graphene, alternatively, by using the electric field of a surface acoustic wave [19]. By means of Keldysh Green's function method and numerical calculations, we demonstrate that the pumped charge current is absent in the low pumping frequency regime and sharply increases as the frequency (ω) matches the Fermi energy of the system, whereas the pumped charge current is always absent in the GNR with armchair edges and the ZGNR with an odd number of zigzag chains since the later systems remain SIS. The two-parameter charge pump in the ZGNR is also studied and the magnitudes are comparable when

the frequency matches the Fermi energy. The spin polarization of the edge state due to Coulomb interaction is neglected, since it is not expected to lead to charge current polarization.

This paper is organized in the following way. In section 2, we introduce the quantum parametric pump in the ZGNR and describe the Keldysh formulae to calculate the pumped current. In section 3, we present the numerical results and discussions of the pumped current. A conclusion is drawn in section 4.

2. Model

We consider a uniform ZGNR in figure 1 that consists of a scattering region and two ideal leads, the pumping potentials are applied on the scattering region with the size $N \times M$, where N is the number of the transverse zigzag chains, M is the number of longitudinal slices in the scattering region, and N is taken as an even number since the odd number ZGNR cannot lead to a pumped current as stated below. The system is absent of any bias so the electrochemical potential is equal everywhere. The single-band (π band) tight-binding Hamiltonian of the ZGNR reads

$$\mathcal{H}_0 = \sum_l \epsilon_l C_l^\dagger C_l + \sum_{\langle l, l' \rangle} t_{ll'} C_l^\dagger C_{l'}, \quad (1a)$$

$$\mathcal{H}_1 = \sum_{i \in S} v_i \cos(\omega t + \phi_i) C_i^\dagger C_i, \quad (1b)$$

where $C_{l(i)}^\dagger$ ($C_{l(i)}$) is the creation (annihilation) operator of electron at site $l(i)$, ϵ_l is the on-site energy, $t_{ll'}$ is the hopping energy of the electron and $\langle l, l' \rangle$ denotes the summation over the nearest-neighbor sites; \mathcal{H}_0 describes the uniform ZGNR including both the ideal leads and the scattering region. To keep the discussion general, \mathcal{H}_1 describes the time-dependent pumping potentials in the scattering region with different pumping strengths v_i and different phases ϕ_i , the summation over $i \in S$ denotes the pumping potentials are confined in the sample region. In a realistic situation, the potentials with the frequency ω are in the same phase and strength, $\phi_i = \phi_0$ and $v_i = v_0$, when a single AC gate voltage is applied to

the system, thus this device is actually referred to as a single-parameter quantum pump. When there is a phase difference between the pumping potentials, it is defined as two-parameter charge pump in this work. The system considered here is impurity free and the generalization to the disordered case is straightforward by including random site energies. We focus on the time average current flowing in the $\alpha = \text{L, R}$ lead, which is given by ($e = \hbar = 1$)

$$I_\alpha = -\frac{1}{\tau} \int_0^\tau dt \int dt_1 \text{Tr}[G^r(t, t_1) \Sigma_\alpha^<(t_1, t) + G^<(t, t_1) \Sigma_\alpha^a(t_1, t) + \text{h.c.}], \quad (2)$$

where τ is the period of the pumping cycle, the trace is over the transverse modes of the ZGNR; $G^{r,a,<}(t, t_1)$ are the retarded (r), advanced (a), and lesser ($<$) Green's functions in the scattering region defined respectively as

$$G_{ll'}^{r(a)}(t, t') = \mp i \theta(\pm t \mp t') \langle [C_l(t), C_{l'}^\dagger(t')] \rangle, \quad (3)$$

$$G_{ll'}^<(t, t') = i \langle C_l^\dagger(t) C_{l'}(t') \rangle, \quad (4)$$

where $\langle \dots \rangle$ denotes the quantum statistic average and $\theta(\pm t \mp t')$ is a step function. $\Sigma_\alpha^{r,a,<}$ is the retarded, advanced, and lesser self-energy from lead α , $\Sigma_\alpha^< = (\Sigma_\alpha^a - \Sigma_\alpha^r) f_\alpha$, f_α is the Fermi Dirac distribution function of lead α , and $f_L = f_R = f$ due to the zero bias applied on the system. The self-energy $\Sigma_\alpha^{r,a}$ can be readily evaluated from the surface Green's function of the ideal leads that are absent of any scattering potentials. To simplify our derivation, a perturbation method is employed to evaluate the Green's function $G^{r,a,<}$ in the sample region and the time-dependent pumping potential \mathcal{H}_1 is taken as the perturbed term. In order to obtain the lesser Green's function $G^<$, we choose first to work out the Green's function in Keldysh space G^k [20] and the following Dyson equation can be used in the calculation,

$$G^k(t, t') = G^{k0}(t, t') + \int dt_1 G^{k0}(t, t_1) V^k(t_1) G^{k0}(t_1, t') + \dots, \quad (5)$$

where $G^k(t, t')$ is the Green's function in Keldysh space, which is defined as [21]

$$G^k(t, t') = \begin{pmatrix} G^t(t, t') & G^<(t, t') \\ G^>(t, t') & G^{\bar{t}}(t, t') \end{pmatrix}, \quad (6)$$

where

$$G^t(t, t') = -i\theta(t - t') \langle C(t) C^\dagger(t') \rangle + i\theta(t' - t) \langle C^\dagger(t') C(t) \rangle, \quad (7)$$

$$G^>(t, t') = -i \langle C(t) C^\dagger(t') \rangle, \quad (8)$$

and

$$G^{\bar{t}}(t, t') = -i\theta(t' - t) \langle C(t) C^\dagger(t') \rangle + i\theta(t - t') \langle C^\dagger(t') C(t) \rangle \quad (9)$$

are the time-order, greater, and anti-time-order Green's function, respectively. The perturbation potential V^k in the Dyson equation is also in the Keldysh space defined as

$$V^k(t) = \begin{pmatrix} \mathcal{H}_1 & 0 \\ 0 & -\mathcal{H}_1 \end{pmatrix}. \quad (10)$$

Here the time-order and anti-time-order components take the plus and minus perturbation potential, whereas the other two components are zero because, as in most cases, the perturbation potential is instantaneous. The four component Green's functions of G^k are not fully independent and they have relations [21] such as

$$G^t = G^< + G^r, \quad (11)$$

$$G^{\bar{t}} = G^< - G^a, \quad (12)$$

and

$$G^> = G^t - G^a. \quad (13)$$

The unperturbed Green's function $G^{k(r)0}$ can be easily worked out since there is no bias and no pumping potentials, i.e., $G^{r0}(E) = 1/(E + i0^+ - \mathcal{H}_0)$ and \mathcal{H}_0 can be replaced by the Hamiltonian of the scattering region plus the self-energy Σ^r from the two leads, since only the Green's function in the scattering region is needed to evaluate the current in equation (2). The unperturbed lesser Green's function is given by $G^{<0} = [G^{a0}(E) - G^{r0}(E)]f$, with f being the Fermi distribution function, thus the G^{k0} can be calculated by using equations (10)–(12). With these preparations and straightforward algebra, we obtain the bilinear response of the pumped charge current in lead α as

$$I_\alpha = -i \sum_{i,j \in S} \frac{v_i v_j}{4} \int d\epsilon \text{Tr}[\Gamma^\alpha(\epsilon) \mathbf{X}^{i,j}(\epsilon)] \times \{ [f(\epsilon + \omega) - f(\epsilon)] [G_{ij}^{r0}(\epsilon + \omega) - G_{ij}^{a0}(\epsilon + \omega)] e^{i\Delta\phi_{ij}} + [f(\epsilon - \omega) - f(\epsilon)] [G_{ij}^{r0}(\epsilon - \omega) - G_{ij}^{a0}(\epsilon - \omega)] \times e^{-i\Delta\phi_{ij}} \}, \quad (14a)$$

$$\mathbf{X}_{m_2, m_1}^{i,j}(\epsilon) = G_{m_2, i}^{r0}(\epsilon) G_{j, m_1}^{a0}(\epsilon), \quad (14b)$$

where the phase difference $\Delta\phi_{ij} = \phi_i - \phi_j$, the line-width function Γ depends on the self-energy: $\Gamma = i(\Sigma^r - \Sigma^a)$, and $m_{1(2)}$ are the indices of the transverse sites of a slice in graphene. This pumped charge formula at a finite frequency is same as that derived from other methods such as the scattering method [22, 23]. By using the identity $G^r - G^a = -iG^r\Gamma G^a$, it is not difficult to verify the conservation of the pumped current as $\sum_\alpha I_\alpha = 0$. From the formula above, the charge current stems from the quantum interference effect between the photon-emission and photon-absorption processes, in the adiabatic regime $\omega \rightarrow 0$, the pumped current is proportional to the pumping frequency, $I_\alpha \sim \omega \sin \Delta\phi_{ij}$, so that the single-parameter pump cannot work and $I_\alpha = 0$ when $\Delta\phi_{ij} = 0$; while in the nonadiabatic regime $\omega \gg 1/\tau$, with τ a characteristic time taken for an electron to traverse the sample, the single-parameter pump can lead to a nonzero current when the system does not possess SIS and the photon-emission and photon-absorption are asymmetric, and $I \sim \omega^2$. Our following calculations are based on the current formula equation (14) above.

3. Calculation and discussion

In this section, we present the numerical results of the pumped current in the ZGNR with the pumping potentials applied

on the scattering region, and these pumping potentials on each lattice point are assumed to be identical, with the same pumping strength and phase. The calculations are carried out at zero temperature $T = 0$ K, the sample region in most cases is taken as a square lattice 20×20 (the qualitative results are independent of the lattice sizes chosen), the site energy is $\epsilon_l = 0$ eV and the hopping energy is $t = -3.0$ eV, the strength of the pumping potential is set as $v_i = 0.01$ eV, that is much smaller than the Fermi energy of graphene to justify the perturbation theory employed in this work. In the experiment, the typical concentration of electrons or holes is around 10^{13} cm^{-2} , so that the Fermi energy corresponds to an order of magnitude of 0.1 eV or so. In this range of energy, the energy dispersion relation of the quasiparticle is linear and exhibits Dirac behavior.

We first consider the single-parameter pump case, where there is no phase difference among these time-dependent pumping potentials. The pumped current I_p in the left lead ($\alpha = L$) is plotted in figure 2 as a function of the pumping frequency ω for different Fermi energies. When the pumping frequency is less than the Fermi energy $\omega < E_F$, the pumped current is almost vanishing; when the frequency increases to $\omega = E_F$, the pumped current rapidly increases to a maximum and then begins to damp. For different E_F , the damping curves with $\omega > E_F$ overlap. The current for the single-parameter pump $\Delta\phi_{ij} = 0$ is an even function of the frequency ω , $I_p(\omega) = I_p(-\omega)$, which can be seen from the current formula of equation (14). The pumped current direction is determined by the Fermi energy being above or below the Dirac point, $I_p(E_F) = -I_p(-E_F)$ can be exactly verified as the symmetric valence and conduction band is considered for the ZGNR, which is related to the fact that the pumped current stems from the quantum interference between the photon-absorption and photon-emission, and the carrier is changed from an electron to a hole (quasiparticle) when Fermi energy is lowered from the conduction band to the valence band, in other words, the pumped current direction is different for n-doped and p-doped ZGNRs.

The nonzero charge current in figure 2 is attributed to the peculiar zero-energy edge state in the ZGNR and the symmetry breaking between A and B carbon atoms at the two edges of the ZGNR. Although there are no impurities or static potential in the sample region where the time-dependent pumping potentials locate, and the unperturbed system is a uniform ZGNR possessing translational symmetry along the longitudinal direction, the inequivalent A and B carbon atom at the edges can lead to the ZGNR with an even number of zigzag chains N lacking SIS, which can be seen from the inversion operation of the scattering region over the central point of the device or the rotation operation by π around the normal of graphene. It is emphasized that when the device is rotated along the longitudinal direction by π , the system remains invariant and one cannot realize an exchange of A carbon and B carbon atoms. From this symmetry analysis, the ZGNR with an odd number of zigzag chains cannot lead to a pumped current, since the spatial structure of the device keeps invariant under the central inversion operation. As a matter of fact, we have also checked the single-parameter pump in another typical

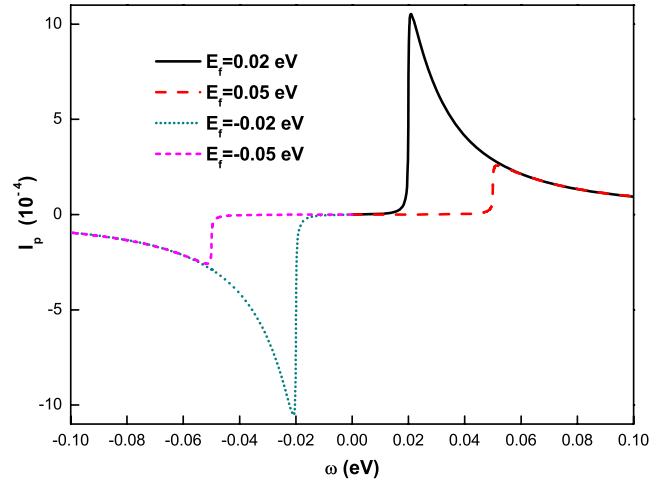


Figure 2. The dependence of the pumped current I_p on the pumping frequency ω for the single-parameter charge pump in the ZGNR. Different curves correspond to different Fermi energies as noted in the panel. The scattering region size is 20×20 , the strength of the pumping potential is set as $v_i = 0.01$ eV.

GNR with armchair edges, and found there is no pumped current, which can also be explained from similar symmetry analysis. This structurally inequivalent property of the ZGNR can lead to a very different transport behavior with an even or odd number of zigzag chain, which was referred to as the odd-even effect of the ZGNR in the literature [24–26], e.g., the Andreev reflection in a superconductor/ZGNR junction with an even number of zigzag chains can be greatly suppressed in contrast to that of an odd number of zigzag chains [24].

In order to clarify the sharp increase of I_p at E_F , we re-express the current formula of a single-parameter pump (equation (14)) at zero temperature as

$$I_\alpha = i \sum_{i,j \in S} \frac{v_i v_j}{4} \int_{E_F - \omega}^{E_F} d\epsilon \mathbf{A}_{ij}(\epsilon) \quad (15)$$

$$\mathbf{A}_{ij}(\epsilon) = \text{Tr}[\Gamma^\alpha(\epsilon) \mathbf{X}(\epsilon) (G_{ij}^{0r}(\epsilon + \omega) - G_{ij}^{0a}(\epsilon + \omega)) - \Gamma^\alpha(\epsilon + \omega) \mathbf{X}(\epsilon + \omega) (G_{ij}^{0r}(\epsilon) - G_{ij}^{0a}(\epsilon))].$$

Since the density of states around the Dirac point is almost zero except for the edge state at $E = 0$, as shown in the inset of figure 3, the integral variable $A(\epsilon) = \sum_{ij} \mathbf{A}_{ij}(\epsilon)$ is only nonzero when the integrand is considered in this energy region. Hence, a nonzero charge current can be pumped out only when the frequency matches the Fermi energy $\omega \sim E_F$ from the lower limit of the integral in the equation above, therefore I_p exhibits an abrupt increase when $\omega = E_F$ in figure 2. As E_F is much closer to the Dirac point, the maximum of I_p is much larger, since in the variable $A(\epsilon)$ (equation (15)) the multiple factors from the $[E_F - \omega, E_F]$ and $[E_F, E_F + \omega]$ regions become larger as $E_F \rightarrow 0$. The magnitude of I_p at $\omega = E_F$ is determined by the broadening of the edge state in the energy gap, which is in turn determined by the impurity level in the ZGNR, so that it is expected that a cleaner material should lead to a larger pumped current. Since the variable $A(\epsilon)$ decreases with ω as seen in figure 3, I_p will decrease as $\omega > E_F$ in figure 2. For different Fermi energies, the damped curves

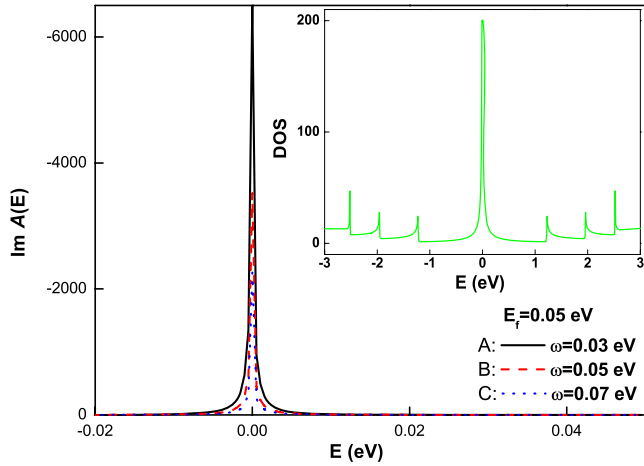


Figure 3. The integral variable $A(\epsilon)$ in equation (15) as a function of the energy E for different pumping frequency ω . The density of states for a unit slice in the ZGNR is plotted in the inset.

of I_p overlap with each other when $\omega > E_F$, this originates from the fact that the integrand $A(\epsilon)$ peaks at $E = 0$, and the whole peak contribution to the integration is fixed as $\omega > E_F$ no matter what E_F is taken.

We proceed to examine the two-parameter charge pump in the ZGNR, the pumping potentials are assumed only at the two boundary slices of the sample region, the left one has a pumping phase ϕ_1 while the right one has a phase ϕ_2 . The charge current I_p is plotted in figure 4 as a function of ω with the phase difference $\Delta\phi = \phi_1 - \phi_2$. The conspicuous feature is the sharp increase of I_p at $\omega = E_F$, and it resembles the tendency of the single-parameter pump. At the resonant point, the pumped currents for both the single- and two-parameter pump have the same order of magnitude, the $\Delta\phi = 0$ case in figure 4 is actually a single-parameter charge pump. The difference is that I_p with $\Delta\phi \neq 0$ begins to increase from $\omega = 0$ and in the adiabatic regime, the I_p is linear in ω ; whereas for $\Delta\phi = 0$, the I_p is nonzero only when ω is comparable to E_F . For these $\Delta\phi \neq 0$ cases, the charge current direction can be also reversed by changing $E_F > 0$ (n-doped) to $E_F < 0$ (p-doped), which indicates the hole–electron antisymmetry of the pumped current. The direction of I_p is certainly dependent on the phase difference $\Delta\phi$, $I_p \sim \sin \Delta\phi$ as shown in the inset of figure 4. Since the nongraphene single-parameter pump results from the breaking of SIS, then the current direction is determined by the relative position of the pumping potential to the leads. For the ZGNR case we study here, the pumped current is determined by the A or B type carbon atoms at one lateral edge besides the E_F locating in the conduction or valence band, it is noted that A or B carbon atoms are just a carbon atom and their difference comes from the topological structure of the actual device, so that some symmetry operations may not exchange A and B atoms or reverse the current direction.

In the calculations above, the Fermi energy E_F is chosen in the energy gap, i.e., it is smaller than the first nonzero transverse energy level. The reason is the weakness of the photon energy $\hbar\omega$ that can lead to $|E_F| < |\omega|$, for the frequency

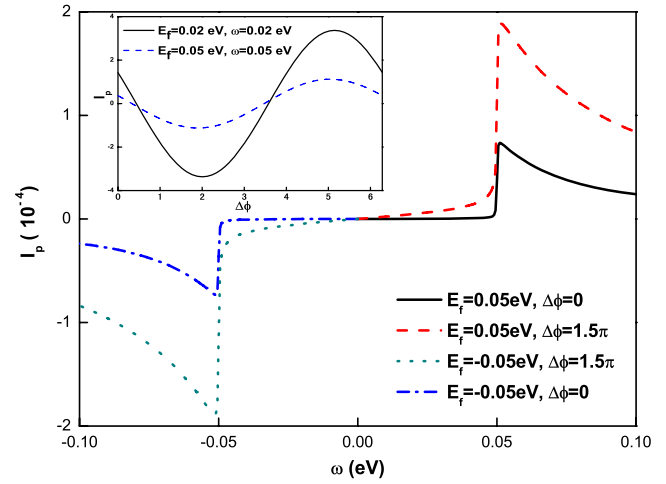


Figure 4. The dependence of the pumped current I_p on the frequency ω of the two-parameter charge pump in a ZGNR for different phase differences. In the inset, the pumped current is presented as a function of the phase difference $\Delta\phi$.

$\omega \sim 1$ GHz the photon energy is about 10^{-2} meV, so that the resonant point $\omega = E_F$ should usually occur in the energy gap of the ZGNR. In fact, the energy gap for a nanoscale ZGNR is comparatively larger than the usual Fermi energy, e.g., a ZGNR with the transverse width 30 nm has an energy gap about 0.1 eV, this is estimated from the energy gap formula $\Delta E = \frac{t\pi}{N+1/2}$, with N the number of the transverse zigzag chains [14]. Therefore, only the edge state at $E = 0$ is considered to contribute to the pumped current in our scheme. Relatively speaking, the experimental realization of a single-parameter charge pump is easier than a two-parameter pump, using either a single AC top gate capacitively coupled to the ZGNR or the electric field of the surface acoustic wave.

Although we consider a clean ZGNR, the weak disorder is not expected to suppress the pumped current by much since the edge state can survive in the weak disorder. However, our findings are much more conspicuous in a cleaner ZGNR because of the lesser broadening of the zero-energy edge state, moreover, the single-parameter pump requires the Fermi energy much closer the Dirac point to satisfy $|\omega| > |E_F|$, thus a lesser doped ZGNR is needed. The key features of the pumped current by a single-parameter pump in a ZGNR are the abrupt increase at $\omega = E_F$ and the reversal of current direction by changing E_F across the Dirac point, which may have potential applications in quantum information technology, e.g., the current I_p can readily be tuned between so-called on and off states by changing the Fermi energy E_F or the frequency ω to match each other. From this perspective, the single-parameter charge pump in the ZGNR is more intriguing than the two-parameter charge pump.

4. Summary

In summary, we have investigated the single-parameter charge pump in a clean ZGNR with no external bias. It was found that a pumped current may flow in a ZGNR with an even number of zigzag chains, whereas it is absent in a ZGNR with

an odd number of zigzag chains as well as in a GNR with armchair edges. The nonzero current in the even-ZGNR can be pumped out only when the pumping frequency matches the Fermi energy of system, and then the pumped current exhibits a sharp increase. The nonzero pumped current results from the zero-energy edge state in an even-ZGNR and the spontaneous symmetry breaking of two inequivalent carbon atoms at the two edges. The current direction can be reversed by alternating the carbon atoms at the two edges or tuning the Fermi energy across the Dirac point. The two-parameter charge pump in the ZGNR retains the main character of the single-parameter pump, and the magnitudes of the two pumped currents are comparable when the pumping frequency matches the Fermi energy. Our findings may be helpful to develop graphene-based electronic devices.

Acknowledgments

The work was supported by the General Research Fund of the Research Grants Council of Hong Kong SAR, China (Project No. CityU 100309/09P); JW thanks support from NSFC (10704016) and NBRPC (2009CB929504); YHY acknowledges support by NSF of JiangSu (BK2007100).

References

- [1] Novoselov K S, Geim A K, Morozov S V, Jiang D, Zhang Y, Dubonos S V, Grigorieva I V and Firsov A A 2004 *Science* **306** 666
- [2] Zhang Y, Tan Y W, Stormer H L and Kim P 2005 *Nature* **438** 201
- [3] Novoselov K S, Geim A K, Morozov S V, Jiang D, Katsnelson M I, Grigorieva I V, Dubonos S V and Firsov A A 2005 *Nature* **438** 197
- [4] Geim A K and MacDonald A H 2007 *Phys. Today* **60** 35
- [5] Castro Neto A H, Guinea F, Peres N M R, Novoselov K S and Geim A K 2009 *Rev. Mod. Phys.* **81** 109
- [6] Beenakker C W J 2006 *Phys. Rev. Lett.* **97** 067007
Beenakker C W J 2008 *Rev. Mod. Phys.* **80** 1337
- [7] Katsnelson M I, Novoselov K S and Geim A K 2006 *Nat. Phys.* **2** 177
- [8] Abanin D A, Lee P A and Levitov L S 2006 *Phys. Rev. Lett.* **96** 176803
- [9] Yang K 2007 *Solid State Commun.* **143** 27
- [10] Heersche H B, Jarillo-Herrero P, Oostinga J B, Vandersypen L M K and Morpurgo A F 2007 *Nature* **446** 56
- [11] Pendry J B 2007 *Science* **315** 1226
Cheianov V V, Fal'ko V and Altshuler B L 2007 *Science* **315** 1252
- [12] Fujita M, Wakabayashi K, Nakada K and Kusakabe K 1996 *J. Phys. Soc. Japan* **65** 1920
- [13] Wakabayashi K, Fujita M, Ajiki H and Sigrist M 1999 *Phys. Rev. B* **59** 8271
- [14] Cresti A, Grosso G and Parravicini G P 2008 *Phys. Rev. B* **77** 115408
- [15] Kobayashi Y, Fukui K I, Enoki T and Kusakabe K 2006 *Phys. Rev. B* **73** 125415
- [16] Brouwer P W 1998 *Phys. Rev. B* **58** R10135
- [17] Wang B G, Wang J and Guo H 2002 *Phys. Rev. B* **65** 073306
- [18] Foa Torres L E F 2005 *Phys. Rev. B* **72** 245339
- [19] Buitelaar M R, Kashcheyevs V, Leek P J, Talyanskii V I, Smith C G, Anderson D, Jones G A C, Wei J and Cobden D H 2008 *Phys. Rev. Lett.* **101** 126803
- [20] Keldysh L V 1965 *Sov. Phys.—JETP* **20** 1018
- [21] Mahan G D 1993 *Many Particle Physics* (New York: Plenum)
- [22] Wang J, Wang B and Xing D Y 2004 *Phys. Lett. A* **326** 449
- [23] Moskalets M and Buttiker M 2002 *Phys. Rev. B* **66** 035306
- [24] Rainis D, Taddei F, Dolcini F, Polini M and Fazio R 2009 *Phys. Rev. B* **79** 115131
- [25] Akhmerov A R, Bardarson J H, Rycerz A and Beenakker C W J 2008 *Phys. Rev. B* **77** 205418
- [26] Wakabayashi K and Oaki T 2002 *Int. J. Mod. Phys. B* **32** 4897